AIAA 79-0646R

Characteristics of Propeller Noise on an Aircraft Fuselage

C. Kearney Barton* and John S. Mixson*
NASA Langley Research Center, Hampton, Va.

Exterior noise was measured on the fuselage of a twin-engine, light aircraft at four values of engine rpm in ground static tests and at forward speeds up to 36 m/s in taxi tests. Propeller noise levels, spectra, and correlations were determined using a horizontal array of seven flush-mounted microphones and a vertical array of four flush-mounted microphones in the propeller plane. The measured levels and spectra are compared with predictions based on empirical and analytical methods for static and taxi conditions. Trace velocities obtained from point-to-point correlations are used to describe the propagating and rotating characteristics of the propeller noise field on the fuselage.

Introduction

PROPELLER noise is one of the major sources of interior noise in many aircraft. Reduction of interior noise in these aircraft requires an understanding of the characteristics of propeller noise for use in studying the resulting noise transmission through the fuselage sidewall.

Propeller noise has been studied in the past, and recent emphasis on communities and passengers has led to renewed interest in understanding propeller noise. Measured levels and spectra are presented by Hubbard and Regier,[1] and a review of technology up to 1970 is presented by Hubbard et al.[2] Recent research has led to the empirical procedures presented by SAE[3] and Ungar et al.[4] for predicting overall levels and spectra, and to the analytical methods presented by Farassat,[5] Farassat and Brown,[6] and Hanson.[7] However, analysis of noise transmission that is detailed sufficiently for accurate prediction of interior noise levels or for development of lightweight noise control treatment requires information on the correlation properties of the noise in addition to the level and spectral properties presented in the references.

The primary purpose of this paper is to describe the level, spectrum, and correlation characteristics of propeller noise impinging on the fuselage of a particular twin-engine, light aircraft. This paper includes information presented by Mixson et al.[8] at the AIAA Aeroacoustics Conference and represents a continuation of the work described in Mixson et al.[9] and Piersol et al.[10,11] Experimentally determined noise characteristics are examined herein and compared with predictions of the empirical methods of Refs. 3 and 4 and with predictions of the analytical method of Farassat[5] and Farassat and Brown.[6]

Aircraft Noise Experiments

The aircraft used in these studies is shown in Fig. 1. Nominally, this aircraft has a takeoff gross weight of 3175 kg, a useful load of 1200 kg, and cruises at an airspeed of 80 m/s at 3050 m altitude with each engine running at 70% power. The range at the most economical cruise speed is 2575 km. Each engine has six cylinders, is rated at 320 hp, and drives a right-handed, 236 cm diam, three-bladed propeller at about 64% of the engine rpm. The propeller plane intersects the fuselage at approximately the middle of the passenger cabin, and the propeller tip clearance from the sidewall is approximately 13 cm. The engine exhaust ports are located near the aft end of the nacelle, near the baggage compartment as indicated in Fig. 1. There are four ports, one on each side of each nacelle, with three cylinders exhausting through each port. The cabin interior was finished in standard trim for this aircraft and provided seats for six passengers including the pilot. The carpet in the passenger section was removed, leaving the floor of bare aluminum. A sample interior noise spectra measured during level flight in this aircraft is shown in Fig. 2.[9] These flight data are included to show the relative importance of the propeller harmonics in the cabin noise level. The spectra was A-weighted so that the highest harmonics represent the most dominant noise sources of A-weighted cabin noise.

The tests described in this paper included static tests with engines running and taxi tests. The static test conditions shown in Table 1 indicate that data were obtained at 4 rpm values with either one or both engines operating. In static

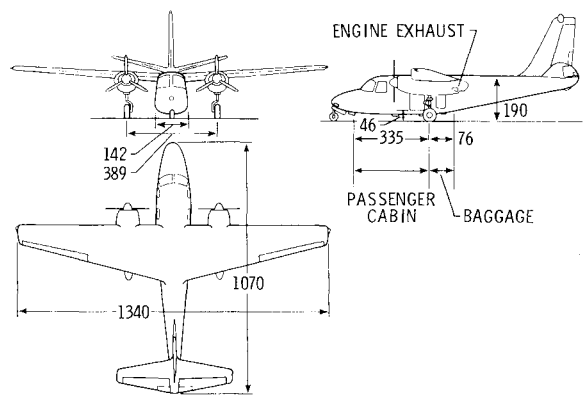

Fig. 1 Sketch of twin-engine, light aircraft used in interior noise studies, dimensions in cm.

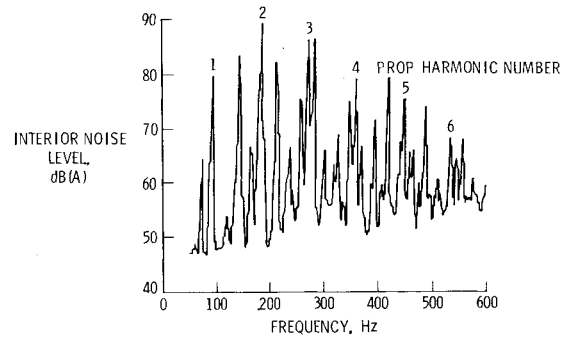

Fig. 2 A-weighted spectrum of interior noise, 75% power, 2750 rpm, 80 m/s.

Presented as Paper 79-0646 at the AIAA 5th Aeroacoustics Conference, Seattle, Wash., March 12-14, 1979; submitted Nov. 13, 1979; revision received July 11, 1980. This paper is declared a work of the U.S. Government and therefore is in the public domain.

*Aero-Space Technologist, Acoustics and Noise Reduction Division. Member AIAA.

tests, the engine rpm was stabilized and records of 30-60 s duration were obtained. The data were taken using 10 precision condenser microphones of 0.6 cm diam mounted flush on the fuselage sidewall in the array shown in Fig. 3. Continuous time histories of instantaneous pressure were recorded on a 14-channel FM tape recorder that was remotely located.

The effect of forward speed on the fuselage sidewall noise for ground conditions was determined from taxi tests. Data were recorded on a 4-channel portable FM tape recorder in the aircraft. The aircraft power and rpm were established with the aircraft held stationary by the brakes; then the tape recorder was turned on and left running as the brakes were released and the aircraft allowed to accelerate to the desired speed, which was held constant by braking. Table 2 indicates speed and rpm values for the taxi tests; for these tests both engines were operating at equal rpm and nominally at 40% power. The propeller pitch was set on the maximum rpm limit (minimum pitch). The table also indicates the locations of the microphones that were recorded on the 4-channel recorder. Segments of the taped noise recorded with the aircraft stationary and with the aircraft taxiing at constant speed were analyzed. Taxi speed was obtained from the aircraft indicated airspeed dial and from a hand-held anemometer located outside the right-hand pilot's window.

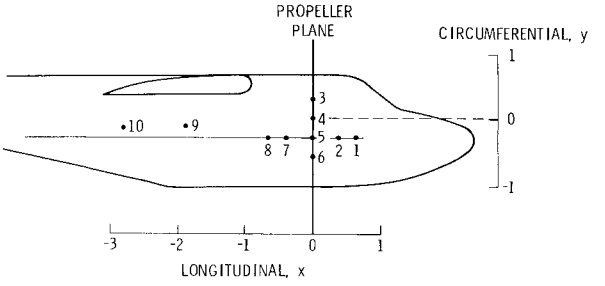

Fig. 3 Nomenclature and coordinates for flush-mounted microphones, coordinates in meters.

Table 1 Static test conditions

Run No.	Engines operating	Engine speed, rpm (nominal)	Engine power hp (each)
1	both	2100	90
2	both	2400	120
3	both	2600	140
4	both	2600	150
5	Stbd	2100	90
6	Stbd	2100	90
7	Stbd	1700	65
8	Stbd	1700	65

Table 2 Taxi test conditions[a]

Run No.	Taxi speed, m/s	Engine speed, rpm (nominal)	Measurement locations[b]
1	0	2600	1,5,8,9
2	15.4	2600	1,5,8,9
3	20.6	2690	1,5,8,9
4	0	2580	3,4,5
5	20.6	2710	3,4,5
6	28.3	2770	3,4,5
7	36	2620	3,4,5

[a] Both engines operating. [b] Shown on Fig. 3.

In each of the setups just described, the overall frequency response was flat within ± 1 dB from below 4 Hz to over 10 kHz and the system signal to noise ratio was at least 40 dB. Details of the analysis of the data are given by Piersol et al.[10] for the static tests and by Piersol et al.[11] for the taxi tests. The wind speed during static tests was less than about 2.2 m/s, but during taxi tests was about 9 m/s, as determined at the weather station adjacent to the test site.

Repeatability of the data can be evaluated, since several of the test conditions were repeated. Table 1 indicates that the following runs were repeated:

Runs:	3 and 4	5 and 6	7 and 8
rpm:	2600	2100	1700
Engines:	Both	Stbd	Stbd

Table 3 shows the harmonic levels for all eight runs for microphone location five. The levels for these pairs of runs are nearly the same, indicating repeatability of most harmonics within about ± 1.5 dB.

Table 1 indicates that runs 1 and 5 had the same rpm, but different engine conditions. Comparison of the data in Table 3 for these two runs indicates that operation of the port engine did not affect the noise measured on the starboard side of the fuselage when the starboard engine was running. From this point in this paper, nonduplicative runs will be discussed; runs 2,4,5, and 7 are emphasized.

Propeller Overall Noise Levels

Static Test Results

The distribution of overall noise level on the fuselage sidewall is shown in Fig. 4 for 2600 rpm. Similar figures are shown in Ref. 8 for 1700, 2100, and 2400 rpm. The data analysis procedures were designed to exclude engine noise, so the measured data in Fig. 4 represent propeller noise. Also

Table 3 Sound pressure levels at propeller harmonics, dB re 20 μPa, location 5, 4 Hz analysis bandwidth

Harmonic order	Run 1	Run 2	Run 3	Run 4	Run 5	Run 6	Run 7	Run 8
1	128.2	131.1	132.6	132.5	127.8	127.8	122.0	121.9
2	121.0	123.7	125.2	125.4	120.3	120.2	116.0	115.9
3	117.4	121.0	122.3	122.2	117.7	117.0	112.2	111.1
4	116.0	119.8	120.4	119.8	113.8	113.8	108.5	108.4
5	111.4	114.2	117.5	117.0	110.8	109.6	105.6	104.2
6	107.9	111.2	115.5	114.7	107.7	106.9	104.3	103.9
7	106.8	109.8	113.1	112.6	106.0	105.7	98.1	97.7
8	102.6	105.2	109.3	109.6	102.2	101.5	99.8	97.7
9	99.5	103.9	106.9	106.6	100.7	99.8	94.8	94.8
10	98.0	101.5	102.5	102.4	98.3	97.2	91.7	90.2
11	96.7	97.3	102.1	102.5	97.2	96.7	86.8	89.6
12	93.4	97.5	99.3	100.8	95.5	95.0	87.9	88.5
13	92.5	97.1	98.8	99.4	93.5	93.4	86.2	86.1
14	91.3	94.0	95.1	96.7	92.8	94.1	84.9	88.1
15	91.3	93.5	96.0	96.6	92.9	93.4	82.5	86.1

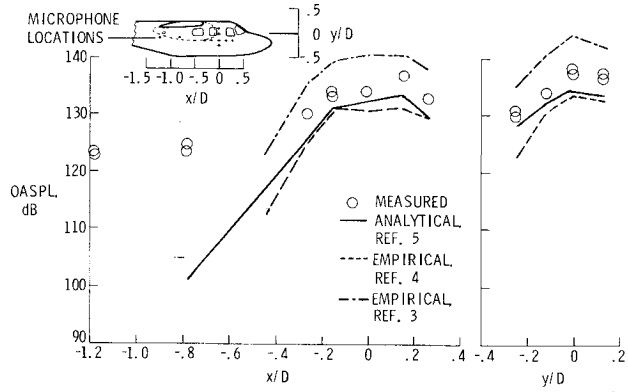

Fig. 4 Distribution of measured and predicted propeller overall noise levels, static condition, 2600 rpm.

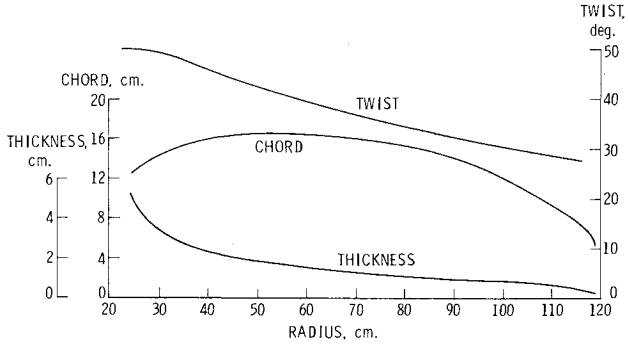

Fig. 5 Distribution of propeller blade dimensions.

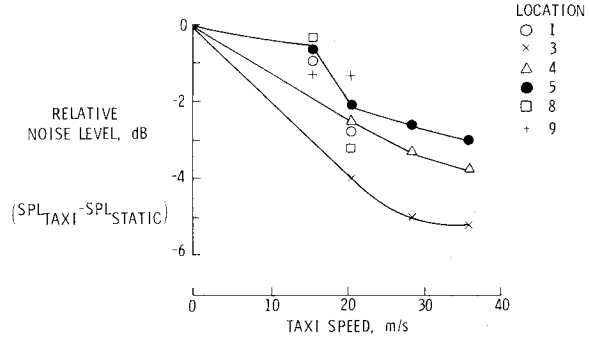

Fig. 6 Variation of propeller overall noise level with taxi speed, 2600 rpm.

shown are levels predicted using the empirical methods of SAE[3] and Ungar et al.[4] and using the analytical method of Farassat.[5] The application of Farassat[5] to the present conditions is described in Ref. 8 for the propeller dimensions shown in Fig. 5. The overall shapes of the predicted distributions are in approximate agreement with the measured shape except at the aft locations $x/D=0.78$ and $x/D=-1.18$. The differences at these aft locations may be due to the presence of some noise mechanism (such as turbulent inflow noise or propeller wake noise) that is not included in the prediction methods, or to the presence of unwanted engine noise in the data. Near the plane of the propeller, $-0.3<x/D<0.3$, the empirically predicted levels differ from each other by as much as 11 dB, and differ from the data by about 6 dB in most cases, depending on the position. The analytical prediction method of Farassat[5] is consistently closest to the measured data; the agreement suggests that the most important noise generating mechanisms are included in the method. (The method of Farassat[5] predicts noise in a free field, so to obtain the analytical results on the sidewall, an empirical sidewall reflection correction obtained from Ref. 3

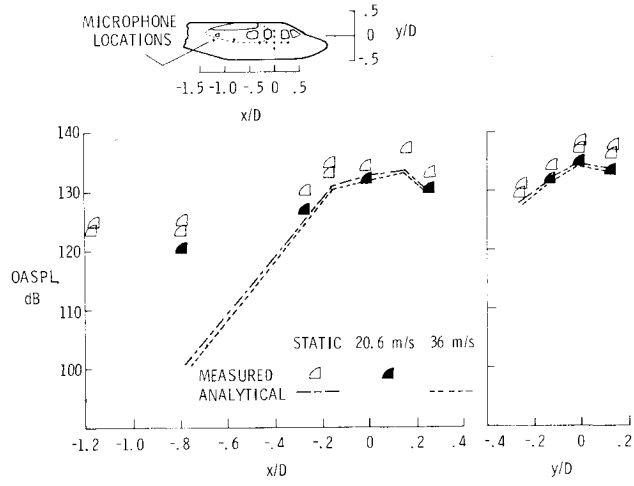

Fig. 7 Distribution of propeller overall noise level for static and taxi conditions, 2600 rpm, 45% power.

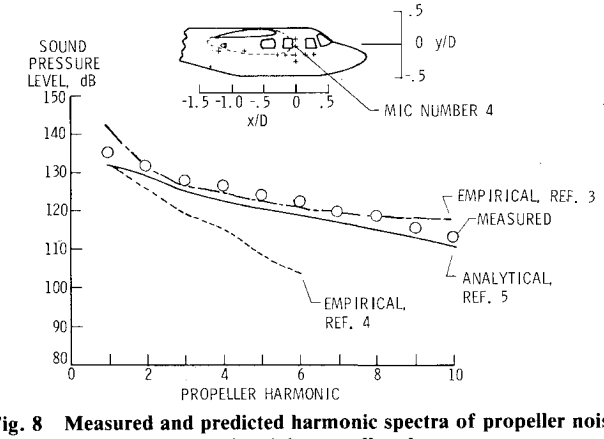

Fig. 8 Measured and predicted harmonic spectra of propeller noise. Static test, 2600 rpm; location 4, in propeller plane.

was added to the free-field level.) The propeller noise level is highest near the propeller plane, $-0.2<x/D<0.2$, and decreases substantially with increasing distance. For example, Fig. 4 shows that the noise level is 10 dB below the maximum value when $x/D\leq -0.5$. In the circumferential direction, the levels also fall rapidly with increasing distance from the point of closest approach of the propeller tip to the sidewall, $y/D=0$. These results suggest that for this tip clearance, noise control treatments might be most effective if located in the sidewall near the propeller plane.

Forward Speed Effects

The effect of forward speed on overall noise level as determined from taxi tests is shown in Fig. 6. In this figure, the SPL at each position is shown relative to the SPL at that position in the static condition. The figure shows that SPL decreases with forward speed, and that the largest decrease measured was about 5 dB at 36 m/s taxi speed. At position 3, the curve appears to be leveling off, suggesting that further reduction of SPL with increasing speed would be small.

The distribution of overall noise level on the fuselage sidewall at 20.6 m/s taxi speed is compared in Fig. 7 with static measurements and analytical predictions. The analytically predicted curves indicate only a slight decrease of OASPL at 36 m/s (the empirical methods do not vary overall sound levels with forward speed). The measured SPL distribution at 20.6 m/s has about the same shape as the static distribution, but the levels are about 3 dB lower. The levels measured near the propeller plane at 20.6 m/s are in close agreement with the analytical predictions of Farassat.[5]

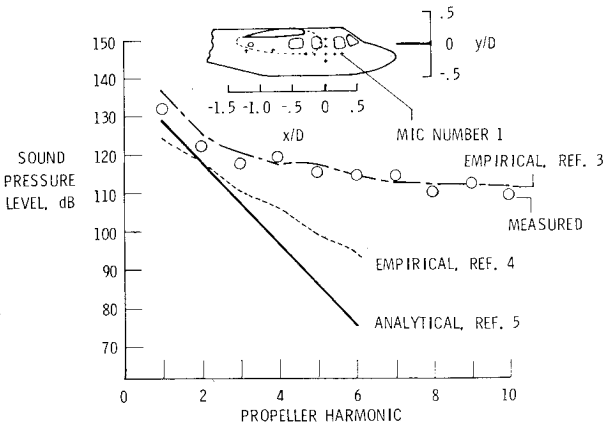

Fig. 9 Measured and predicted harmonic spectra of propeller noise: location 1, forward of propeller plane; static test, 2600 rpm.

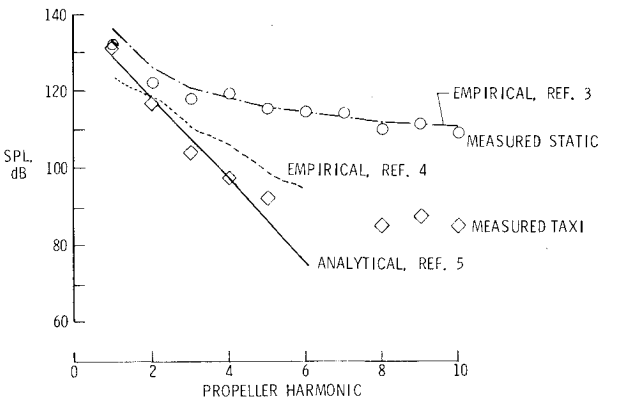

Fig. 11 Comparison of measured and predicted propeller spectra for static and taxi conditions: location 1, $x/D = 0.26$, 2600 rpm, 20.6 m/s taxi.

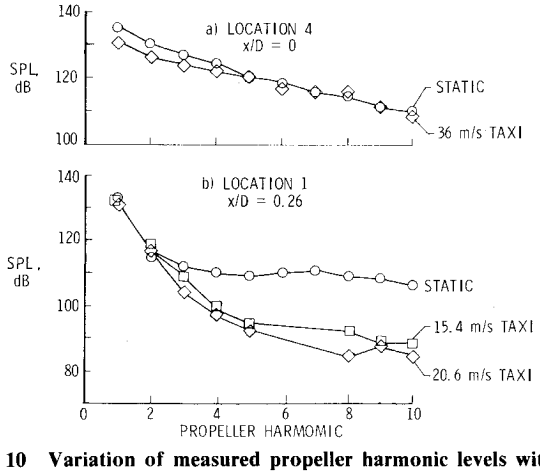

Fig. 10 Variation of measured propeller harmonic levels with taxi speed for two locations, 2600 rpm.

Propeller Noise Spectra

Static Test Results

Levels of propeller harmonics are presented in Figs. 8 and 9 for two locations on the fuselage sidewall for the 2600 rpm static test condition. Figure 8 shows a measured spectrum along with three predicted spectra for the location nearest the edge of the propeller disk. The figure shows that the analytical prediction of Farassat[5] has a spectrum shape that is very close to the measured shape, and that is closer to the measured shape than are the other predictions. The spectrum levels predicted analytically[5] are about 3 dB below the data at all harmonics. The empirical prediction of SAE[3] agrees with the data on average, but is 6.5 dB high at the first harmonic, low at midharmonics, and high by 4 dB at the tenth harmonic. The empirical prediction of Ungar et al.[4] is about 3 dB lower than the data at the first harmonic, but diverges sharply until it is 18 dB lower at the sixth harmonic. The agreement between the measured levels and the analytical predictions[5] suggests that the most important noise generating mechanisms are incorporated in the theory. The measured spectrum falls at about 2.4 dB per harmonic and is down by 17 dB at the seventh harmonic, which might suggest that the lower harmonics are the most significant. However, Mixson et al.[8] showed that the highest interior levels in this aircraft in flight on an A-weighted basis (Fig. 2) occurred between about 160 and 400 Hz corresponding to harmonics from the second to the fourth in Fig. 8. This indicates that many of the harmonics shown may be important for interior noise. Spectra measured and predicted at locations 3 and 4 (the locations closest to the edge of the propeller disk) at all four rpm values closely resemble the corresponding spectra shown in Fig. 8.

Spectra for location 1 are shown in Fig. 9. This location is further from the propeller disk than locations 3 and 4, and the figure shows that the spectrum is different. The analytical prediction of Farassat[5] is still close to the data at the first two harmonics (about 3 dB lower) but then diverges sharply and predicts much lower levels than were measured at higher harmonics. This indicates that a noise mechanism such as the interaction of the in-flow turbulence with the blades, not included in the theory, is important for propeller noise. The empirical method of SAE[3] is close to the data in general, as for Fig. 8, and is about 4 dB higher at the first harmonic. The empirical method of Ungar et al.[4] predicts levels far below the measured, as in Fig. 8. The appearance of the spectra measured and predicted at locations 1,6, and 8 at all four rpm values closely resemble the corresponding spectra in Fig. 9. Figures 8 and 9 indicate that the spectrum shape changes with position relative to the propeller and that different noise generating mechanisms may be dominant in the important range of the higher harmonics. The empirical method of Ref. 3 gives the best overall agreement with the measurements for static conditions. The effects of forward speed change this result, as will be shown in later figures.

Forward Speed Effects

The effect of forward speed on measured spectra as determined from taxi tests is shown in Fig. 10 for two locations on the fuselage sidewall. Figure 10a shows that the effects of forward speed at location 4 is primarily a reduction of about 4 dB in the first three harmonics. The effects of forward speed is similar at locations 3 and 5, i.e., at locations very close to the edge of the propeller disk. At position 1, which is forward of the propeller plane, Fig. 10b shows much greater effects of forward speed. The reductions at the higher harmonics are as large as 24 dB and most of the reduction has occurred when the lower taxi speed of 15.4 m/s has been reached. Similar large reductions at higher harmonics have been reported previously (for far-field noise levels) by Metzger et al.[12] and Pegg et al.,[13] where the cause has been identified as a change of the atmospheric turbulence flowing into and interacting with the propeller.

The reductions of exterior noise shown in Fig. 10b may not result in reductions of interior noise (at least for the present aircraft configuration) because the levels near the propeller, Fig. 10a, remain high as forward speed increases. A comparison of predicted noise levels with measurements at both static and taxi conditions at location 1 is shown in Fig. 11. This figure shows that the data at 20.6 m/s taxi speed is in good agreement with the analytical prediction and in fair agreement with the empirical prediction of Ungar et al.[4]

The comparisons between predicted and measured spectra may be summarized by indicating that the best agreement was obtained by the method indicated in Table 4 for the particular

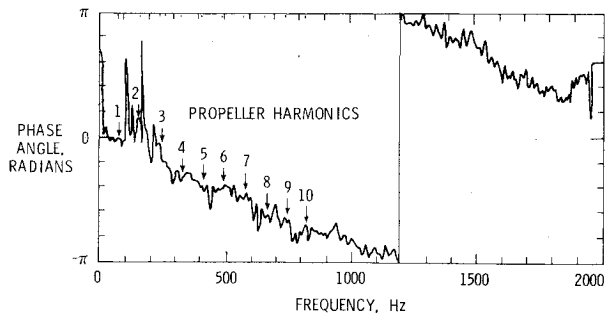

Fig. 12 Sample cross-spectrum phase from narrow-band correlation analyses: locations 1 and 2, run 4, 2600 rpm.

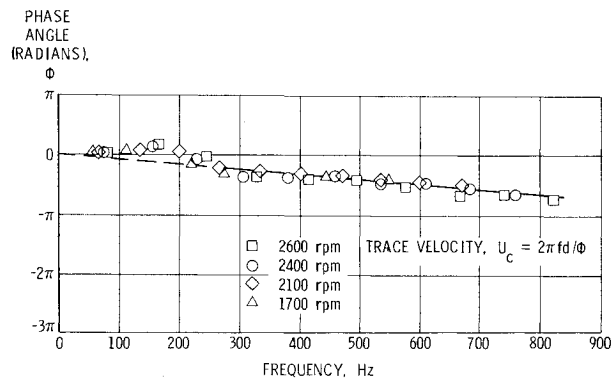

Fig. 13 Variation of cross-spectrum phase angle with frequency for propeller noise components; separation distance between microphones = *d*, longitudinal direction, locations 1 and 2.

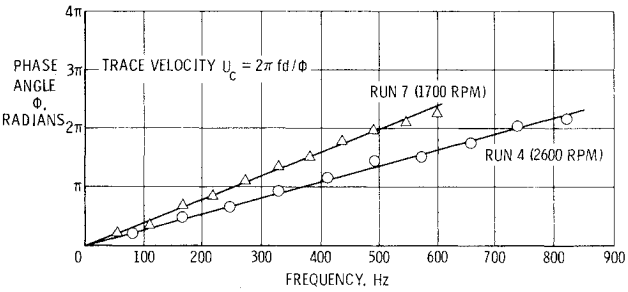

Fig. 14 Variation of cross-spectrum phase angle with frequency for propeller noise components; circumferential direction, *d* = distance between microphones, 0.3 m, locations 4 and 5.

test condition and location indicated. It should be noted that the empirical methods do not contain an explicit correction for forward speed. The correction is through the helical tip Mach number (correction to spectra) but this is small for light aircraft conditions.

Propeller Noise Correlation

Longitudinal Direction

To determine the relation of the acoustic pressures between various locations on the sidewall, coherence and cross-spectrum phase angle between pairs of flush-mounted microphones were determined. Figure 12 shows a sample plot of phase angle as a function of frequency. The primary interest here is the propeller noise, so values of phase angle were determined at the propeller harmonics, adjusted for shifts of 2π such as shown at about 1200 Hz and plotted as shown in Fig. 13. Figure 13 shows values of phase angle between microphones 1 and 2 for four runs at rpm values from 1700 to 2600. The data indicates that the phase angles for all four rpm's lie along the same curve; the solid line has been fitted to the data and to the origin.

Table 4 Preferred prediction methods

	Near propeller $x/D=0, z/D=0.058$	Further from propeller $x/D=0.26, z/D=0.075$
Static	Empirical[3] Analytical[5] (Fig. 8)	Empirical[3] (Fig. 9)
Taxi	Empirical[3] Analytical[5] (Figs. 8 and 10)	Empirical[4] Analytical[5] (Fig. 11)

Table 5 Circumferential convection characteristics

Microphone pair	Run 4 2600 rpm	Run 2 2400 rpm	Run 5 2100 rpm	Run 7 1700 rpm
		Trace velocity; U_c, m/s		
3-4	217	216	180	160
4-5	209	193	171	143
5-6	326	317	244	201
		Velocity ratio, U_c/U_c' [a]		
3-4	0.97	1.05	0.99	1.07
4-5	0.90	0.90	0.90	0.92
5-6	1.22	1.30	1.13	1.14

[a] U_c' = trace velocity of rigid body pressure field.

A value of trace velocity can be determined from the values for phase and frequency for two microphone locations, as indicated by the equation in Fig. 13. The fact that the data points for different harmonics and rpm all fall on a single straight line indicates that the trace velocity is independent of frequency and propeller rpm. Plots of phase angle vs frequency for microphone pairs (7,8), (8,9), and (9,10) also indicated that trace velocity at those areas is independent of frequency and propeller rpm. Note that these microphone pairs lie in a horizontal plane and do not include microphones in the propeller plane. The interpretation of the phase angle diagrams for microphone pairs including one in the propeller plane and one out of the plane is not so straightforward, as discussed in Piersol et al.[10,11]

Circumferential Direction

Phase angles measured for a microphone pair (4,5) in the vertical array are shown in Fig. 14. The data for a given rpm fall on a straight line function of frequency, indicating that the circumferential trace velocity is also independent of frequency. Phase angles for different rpm do not lie on the same line in this case, indicating that trace velocity is dependent on propeller rpm. Values of trace velocity (U_c) are shown in Table 5 as determined from plots such as shown in Fig. 14 for various rpm and microphone pairs in the vertical array. The trace velocities are all subsonic, decrease with decreasing rpm, and vary with microphone pair. A possible hypothesis to explain these data consists of a pressure field that rotates as a rigid body with the propeller. (In a free field, the pressure field does rotate as a rigid body at propeller speed.) Trace velocities U_c' calculated on this model have been used to determine the ratios U_c/U_c' shown in Table 5. The values of velocity ratio range from 0.90 to 1.07 [excluding microphone pair (5,6)] suggesting that the rigid body pressure field may serve as a first approximation model.

Assuming a rotating rigid body pressure field exists, a pressure front, or line of constant phase can be determined as shown in Fig. 15. The data in this figure were determined by calculating the delay time between microphone pairs, calculating the tangential velocity of the assumed rotating field (U_c) at the fuselage, and then estimating the shape by determining the distance traveled at velocity U_c in the delay time for each microphone pair. For example, the velocity between microphones 9 and 10 was 353 m/s resulting in a

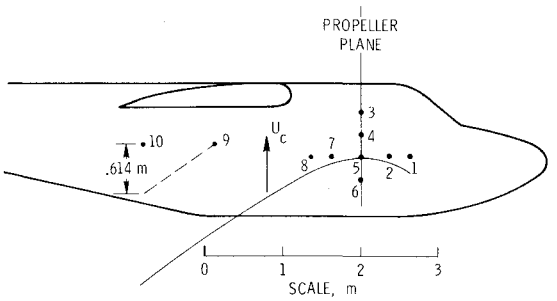

Fig. 15 Impingement geometry of rotating pressure field, 2600 rpm.

travel time of 2.67 ms (distance = 0.994 m) and assuming a rotating pressure field at 2600 rpm, $U_c = 230$ m/s (average measured velocity). Using the rotating field U_c and the delay time, the tangential delay distance is 0.614 m as shown in Fig. 15.[10] Thus, the supersonic trace velocities between longitudinal microphone pairs can be explained by a pressure front rotating with the propeller as shown in Fig. 15.

Concluding Remarks

This paper presents a description of the acoustic field generated by a propeller and impinging on the fuselage sidewall of a twin-engine, light aircraft. An array of 10 flush-mounted microphones was used to measure impinging noise at four combinations of rpm and power in static tests and at speeds up to 36 m/s in taxi tests. Overall levels and harmonic spectra are compared with predictions of two empirical methods and an analytical method, and measured correlation characteristics are described. The analytical method is modified herein to include an empirical correction for the effects of impingement on the fuselage sidewall.

Results indicate that each of the prediction methods agrees with measured levels or spectra in some region of the sidewall, the frequency spectrum, or the forward speed range. The analytical method has the best potential of the three methods studied for providing the noise characteristics needed for accurate noise prediction on the fuselage. It was shown to provide the best agreement with measured overall levels, and to have the flexibility to describe the observed changes of harmonic spectra with position along the sidewall. In addition, analytical methods have the potential capability to describe noise variations with forward speed and point-to-point correlation properties. The analytical method would be further improved by development of analytical corrections for the sidewall reflection effect, inclusion of inflow turbulence noise mechanisms, and prediction and verification of the noise fields for other important configurations, such as those having the fuselage immersed in the propeller wake. Such detailed propeller noise prediction methods would be useful with noise transmission studies to determine the sensitivity of interior noise to variations of propeller characteristics and to determine the best method for combining sidewall and propeller characteristics to minimize interior noise.

Finally, examination of phase angle differences between pairs of microphones led to a description of the correlation properties in terms of a rigid body acoustic pressure field rotating with the propeller.

References

[1] Hubbard, H.H. and Regier, A.A., "Free-Space Oscillating Pressure Near the Tips of Rotating Propellers," NACA Rept. 996, 1950.

[2] Hubbard, H.H., Lansing, D.L., and Runyan, H.L., "A Review of Rotating Blade Noise Technology," Presented at the Aerodynamics Noise Symposium, Leicestershire, England, Sept. 1970.

[3] "Prediction Procedure for Near-Field and Far-Field Propeller Noise," SAE Aerospace Information Rept. AIR 1407, May 1977.

[4] Ungar, E.E., Wilby, J.F., and Bliss, D.B., "A Guide for Estimation of Aeroacoustic Loads on Flight Vehicle Structures," AFFDL-TR-76-91, Vol. I, Feb. 1977.

[5] Farassat, F. "Theory of Noise Generation from Moving Bodies with an Application to Helicopter Rotors," NASA TR R-451, Dec. 1975.

[6] Farassat, F. and Brown, T.J., "A New Capability for Predicting Helicopter Rotor and Propeller Noise Including the Effect of Forward Motion," NASA TM X-74037, June 1977.

[7] Hanson, D.B., "Near-Field Noise of High Tip Speed Propellers in Forward Flight," AIAA Paper 76-565, 3rd AIAA Aeroacoustics Conference, Palo Alto, Calif., July 1976.

[8] Mixson, J. S., Barton, C.K., Piersol, A.G., and Wilby, J.F., "Characteristics of Propeller Noise on an Aircraft Fuselage Related to Interior Noise Transmission," AIAA Paper 79-0646, 5th Aeroacoustics Conference, Seattle, Wash., March 1979.

[9] Mixson, J.S., Barton, C.K., and Vaicaitis, R., "Investigation of Interior Noise in a Twin-Engine Light Aircraft," *Journal of Aircraft*, Vol. 15, April 1978, pp. 227-233.

[10] Piersol, A.G., Wilby, E.G., and Wilby, J.F., "Evaluation of Aero Commander Propeller Acoustic Data: Static Operations," NASA CR-158919, May 1978.

[11] Piersol, A.G., Wilby, E.G., and Wilby, J.F., "Evaluation of Aero Commander Propeller Acoustic Data During Taxi Operations," Bolt Beranek and Newman, Inc., Rept. 3867, Nov. 1978.

[12] Metzger, F.B., Magliozzi, B., and Pegg, R.J., "Progress Report on Propeller Aircraft Flyover Noise Research," SAE Paper 760454, Presented at Business Aircraft Meeting, Wichita, Kan., April 1976.

[13] Pegg, R.J., Magliozzi, B., and Farassat, F., "Some Measured and Calculated Effects of Forward Velocity on Propeller Noise," ASME Paper 77-GT-70, March 1977.